Title

Current definitions of the breathing cycle in alveolar breath-by-breath gas exchange analysis

Journal

AJP Regulatory Integrative and Comparative Physiology, 325(5)

ISSN

0363-6119

Authors

Girardi, Michele
Gattoni, Chiara
Stringer, William W
et al.

Publication Date

2023-11-01

DOI

10.1152/ajpregu.00065.2023

Peer reviewed

Current definitions of the breathing cycle in alveolar breath-by-breath gas exchange analysis

Michele Girardi[1,2*], Chiara Gattoni[1,3], William W. Stringer[1], Harry B. Rossiter[1], Richard Casaburi[1], Carrie Ferguson[1] and Carlo Capelli[3]

[1] The Lundquist Institute for Biomedical Innovation at Harbor-UCLA Medical Center, Torrance, CA, USA. [2] School of Sport, Rehabilitation and Exercise Sciences, University of Essex, Wivenhoe Park, Colchester, UK. [3] Department of Neuroscience, Biomedicine and Movement Sciences, University of Verona, Verona, Italy.

***Corresponding Author:** Michele Girardi, PhD, Institute of Respiratory Medicine and Exercise Physiology, Division of Respiratory and Critical Care Physiology and Medicine, The Lundquist Institute for Biomedical Innovation at Harbor-UCLA Medical Center, Torrance, CA, USA; Phone: +1 (310) 222-8200; e-mail: michele.girardi@lundquist.org. Carlo Capelli, MD, Department of Neuroscience, Biomedicine and Movement Sciences, University of Verona, Verona, Italy; e-mail: carlo.capelli@univr.it.

ORCID iDs

Michele Girardi https://orcid.org/0000-0001-8102-7384

Chiara Gattoni https://orcid.org/0000-0002-7372-7484

William W Stringer https://orcid.org/0000-0003-2756-6728

Harry B Rossiter https://orcid.org/0000-0002-7884-0726

Richard Casaburi https://orcid.org/0000-0002-8851-8589

Carrie Ferguson https://orcid.org/0000-0001-5235-1505

Carlo Capelli https://orcid.org/0000-0002-3278-1337

Submission Type: Review Article

Running head title: Definitions of the human breathing cycle

Text-only word count: 6604

Number of references: 66

Numbers of Figures: 6

Numbers of Tables: 1

Abstract word count: 220

ABSTRACT

Identification of the breathing cycle forms the basis of any breath-by-breath gas exchange analysis. Classically, the breathing cycle is defined as the time interval between the beginning of two consecutive inspiration phases. Based on this definition, several research groups have developed algorithms designed to estimate the volume and rate of gas transferred across the alveolar membrane ("alveolar gas exchange"); however, most algorithms require measurement of lung volume at the beginning of the i^{th} breath (V_{Li-1} – i.e., the end-expiratory lung volume of the preceding i^{th} breath). The main limitation of these algorithms is that direct measurement of V_{Li-1} is challenging and often unavailable. Two solutions avoid the requirement to measure V_{Li-1} by redefining the breathing cycle. One method defines the breathing cycle as the time period between two equal fractional concentrations of lung expired oxygen (F_{O_2}) (or carbon dioxide; F_{CO_2}), typically in the alveolar phase, whereas the other uses the time period between equal values of the F_{O_2}/F_{N_2}(or F_{CO_2}/F_{N_2}) ratios. Thus, these methods identify the breathing cycle by analyzing the gas fraction traces rather than the gas flow signal. In this review, we define the traditional approach and two alternative definitions of the human breathing cycle and present the rationale for redefining this term. We also explore the strengths and limitations of the available approaches and provide implications for future studies.

Keywords: Respiratory cycle, gas exchange, kinetics, exercise, cardiopulmonary exercise testing, lung gas stores

Introduction

Identification of the breathing cycle forms the basis of the quantitative analysis of alveolar breath-by-breath (B-by-B) gas exchange (1, 2). Classically, the breathing cycle is identified by analyzing the gas flow signal from a flow meter, where the zero-crossing points represent the transition between inspiratory and expiratory phases, and vice versa. The gas flow, together with the gas fractions, are generally collected at the mouth and used to estimate alveolar gas exchange on a B-by-B basis. However, accurate and reliable estimation of gas transfer across the alveolar membrane ($\dot{V}O_{2A}$ and $\dot{V}CO_{2A}$) requires changes in B-by-B lung gas stores to be known (2).

Several research groups have developed algorithms and methods to estimate the B-by-B alveolar gas exchange; however, most algorithms require knowledge of the absolute lung volume at the beginning of the i^{th} breath (V_{Li-1}; i.e., the end-expiratory lung volume of the preceding i^{th} breath) (3–8). Due to the technical complexity of measuring V_{Li-1}, it is generally estimated rather than measured directly (9, 10). However, different values of V_{Li-1} lead to different B-by-B alveolar gas exchange estimations (11). In addition, V_{Li-1} is not stable during exercise (7, 12) and is affected by body position (13) and exercise modality (e.g., walking, running, and cycling) (14). Therefore, the validity of these techniques depends largely on the validity of the V_{Li-1} measurement.

Grønlund (15) conceived an ingenious solution to overcome the issues related to the determination of V_{Li-1}; however, this solution required redefining the breathing cycle. In Grønlund's algorithm a single breathing cycle is identified between two points on successive, but not necessarily consecutive, breaths with the same fractional concentration (or partial pressure) of lung O_2 (or CO_2) occurring typically in the alveolar phase (F_{O_2} or F_{CO_2}). Intra-breath integration of gas flow and concentration fractions is performed between these two points, allowing the estimation of alveolar gas exchange without the need for V_{Li-1} measurement (see below). A modification of this technique has been proposed by Cettolo and Francescato that also eliminates need to measure

V_{Li-1}, but uses a different redefinition of the breathing cycle (16). This algorithm (16) defines the breathing cycle as the time interval elapsed between two successive, but not necessarily consecutive, breaths with the same fractional concentration of lung O_2/N_2 (or CO_2/N_2) ratio, typically in the alveolar phase (F_{O_2}/F_{N_2}or F_{CO_2}/F_{N_2}). Therefore, these two techniques use gas fractional concentration signals instead of gas flow signals to define the breathing cycle (Table 1).

This review presents the current definitionss of the human breathing cycle and provides the rationale behind the use of alternative definitions, which arises from the need to estimate alveolar gas exchange. A brief description of gas exchange measurements at the mouth level is provided to facilitate the understanding of different alveolar corrections (more in-depth information on mouth measurements can be found elsewhere (1, 2, 4, 17–19)). Moreover, we summarize the main limitations of applying one technique over another and present implications for future research. We have focused our review on definitions of the breathing cycle using B-by-B open-circuit systems that measure the inspired and expired gas flows and volumes. Historical perspectives of the development of B-by-B gas exchange analysis, including details of the equipment, measurements, and volume and gas corrections, are available elsewhere (1, 2, 4, 17–25).

TABLE 1 NEAR HERE

The classical definition of the breathing cycle for B-by-B gas exchange analysis

Remarkable developments in real-time B-by-B open-circuit systems during the second half of the 20th century made it possible to quantify the inspired and expired gas volumes in real-time (1, 18, 20). The breathing cycle was identified based on these techniques and used to quantify external respiration (i.e., exchange of O_2 and CO_2 between the alveoli and pulmonary capillary) on a B-by-B basis.

In general, a cycle can be defined as a series of incidences of the same condition that are repeated over time. Accordingly, the breathing cycle can be defined as the time interval between two equal incidences (i.e., inspiration or expiration phases). Convention defines "a breath" from the time interval between the beginning of two consecutive inspiration phases (Figure 1).

FIGURE 1 NEAR HERE

The first step in identifying the breathing cycle is to detect the beginning and end of each inspiration and expiration phase. This requires analysis of the gas flow signal ($\dot{V}$) from the flow meter. Theoretically, zero-crossing points of the flow signals can be used to identify the start and end of each inspiration and expiration phase, as the sign of the flow signal changes with inhalation and exhalation (Figure 1). However, the flow signal, being a digitalized signal, rarely presents an absolute zero value. Therefore, the nearest points to zero in the flow signal are generally used in B-by-B gas exchange analysis to provide a reasonable estimation of the transition points between inspiration and expiration, and vice versa (12).

Determining the beginning and end of each inspiration and expiration phase enables the estimation of the inspiratory and expiratory volumes. The volume of the inspired (V_{in}) and expired (V_{ex}) gas is determined by integrating the flow signal during the inspiration and expiration phases of the i^{th} breath, respectively.

$$V_{in_i} = \int_{t_{bi_i}}^{t_{ei_i}} \dot{V}_{in} \cdot \mathrm{d}t \quad (1)$$

$$V_{ex_i} = \int_{t_{be_i}}^{t_{ee_i}} \dot{V}_{ex} \cdot \mathrm{d}t \quad (2)$$

where t_{bi_i} and t_{ei_i} are the time instants at which the inspiration phase begins and ends of breath *i*, respectively, whereas t_{be_i} and t_{ee_i} are the time instants at which the expiration phase begins and ends for the i^{th} breath, respectively. The total time (t_{TOT}) over the i^{th} breath can be defined as $t_{TOT_i} = t_{in_i} + t_{ex_i}$, where t_{ex_i} and t_{in_i} are the expiratory and inspiratory times, respectively.

It is then possible to derive other important ventilatory-based variables over a breathing cycle, such as tidal volume (V_T), breathing rate (B_R), expired flow ($\dot{V}_E$), and inspired flow ($\dot{V}_I$) from V_{ex_i}, V_{in_i}, t_{ex_i}, and t_{in_i}. V_T, B_R, $\dot{V}_E$, and $\dot{V}_I$ (commonly expressed in L·min^{-1} for $\dot{V}_E$ and $\dot{V}_I$, breaths·min^{-1} for B_R, and L for V_T) for each breath from this flow signal (see (1, 4, 17, 25) for the relevant equations).

Several commercial automated B-by-B systems do not compute V_{in} (and the associated $\dot{V}_I$) directly. Instead, these variables are estimated using the nitrogen balance approach: $V_{in} \cdot F_{IN_2} = V_{ex} \cdot F_{EN_2}$ (i.e., the so-called Haldane's correction; reviewed in Ward, 2018)), where F_{IN_2} and F_{EN_2} are the mean fractions of nitrogen (N_2) during the inspiration and expiration phases, respectively.

$$V_{in} = V_{ex} \cdot \frac{F_{EN_2}}{F_{IN_2}} \quad (3)$$

Since B-by-B systems generally also do not measure the N_2 fraction directly, and as there is only a negligible quantity of other inert gases in the inspired air, F_{N_2} is commonly estimated as follows: $F_{N_2} = 1 - (F_{O_2} + F_{CO_2})$. Accordingly, $\dot{V}_I$ for breath *i* can be determined as follows:

$$\dot{V}_{I_i} = \dot{V}_{E_i} \cdot \frac{1 - F_{EO_{2i}} - F_{ECO_{2i}}}{1 - F_{IO_{2i}} - F_{ICO_{2i}}} \quad (4)$$

However, this Haldane correction is intrinsically flawed when applied to B-by-B gas exchange analysis, as it assumes constancy in the lung N_2 stores, which, over the duration of a single breathing cycle, occurs only when the breathing exchange ratio (RER = $\dot{V}CO_2/\dot{V}O_2$) is equal to 1 and consecutive end-expiratory lung volumes are precisely equal (2). Fluctuations in the end-expiratory lung volume at rest (29) and during exercise (7) cause subsequent changes in the fractional composition of the lung gas. Therefore, to facilitate accurate alveolar gas exchange measurement, $\dot{V}_I$ should be measured directly.

Identifying the beginning and end of the inspiration and expiration phases of breath *i* also enables quantification of the volumes of the inspired and expired gas. The total volume of O_2 and CO_2 exchanged at the mouth over the i^{th} breath (VO_{2iM} and VCO_{2iM}, respectively) is determined by the difference between their inspired and expired volumes.

$$VO_{2_iM} = \int_{t_{bi_i}}^{t_{ei_i}} F_{IO_2} \cdot \dot{V}_{in} \cdot \mathrm{d}t - \int_{t_{be_i}}^{t_{ee_i}} F_{EO_2} \cdot \dot{V}_{ex} \cdot \mathrm{d}t \quad (5)$$

$$VCO_{2_iM} = \int_{t_{be_i}}^{t_{ee_i}} F_{ECO_2} \cdot \dot{V}_{ex} \cdot \mathrm{d}t - \int_{t_{bi_i}}^{t_{ei_i}} F_{ICO_2} \cdot \dot{V}_{in} \cdot \mathrm{d}t \quad (6)$$

where F_{IO_2} and F_{EO_2} are the instantaneous O_2 fractions in the inspired and expired gas of breath *i*, and F_{ICO_2} and F_{ECO_2} are the instantaneous CO_2 fractions in the inspired and expired gas over the i^{th} breath, respectively. Therefore, the intra-breath integration of flow and gas tensions is performed over the inspiration and expiration phases of breath *i*, from which the volumes of O_2 and CO_2 exchanged at the mouth during a single breathing cycle are obtained (Figure 1 depicts gas flow (panel A), and O_2, and CO_2 gas tension traces (panel B and C, respectively) used to perform the intra-breath integration).

Some studies have shown that the use of VO_{2M} instead of VO_{2A} amplifies the intrinsic B-by-B variability in O_2 exchange (2, 5–7, 10, 12). Similar results were expected for the difference between the B-by-B variability of VCO_{2M} and VCO_{2A}, although the B-by-B variability for the alveolar CO_2 exchange could be greater than for O_2 exchange (5). In contrast, the average values of VO_{2M} and VCO_{2M} during steady-state conditions can be considered an unbiased average of the alveolar gas exchange (i.e., VO_{2A} and VCO_{2A}) (7, 10, 12). However, the differences between external gas exchange measured at the mouth and that between the alveolar space and pulmonary capillary can be substantial during the work rate transition phases (4, 30), as neither Equations 5 nor 6 consider the changes in the volumes of each gas stored in the lung. Therefore, distinguishing between gas exchange at the mouth and the alveoli under these conditions is of paramount importance.

Several approaches designed to estimate VO_{2A} and VCO_{2A} from measurements of gas volumes exchanged at the mouth have been proposed (for a complete review, please see Capelli et al. (2)). Each of these approaches derives from the pioneering work of Auchincloss et al. (3). The alveolar-capillary gas transfer over breath *i* differs from the transfer measured at the mouth by the changes in the lung gas stores over the same breath:

$$VO_{2_iA} = VO_{2_iM} - \Delta VO_{2_iS} \quad (7)$$

$$VCO_{2_iA} = VCO_{2_iM} + \Delta VCO_{2_iS} \quad (8)$$

where ΔVO_{2_iS} and ΔVCO_{2_iS} represent the changes in the volumes of O_2 and CO_2 stored in the lung, respectively. The net transfer of O_2 or CO_2 at the alveolar level approaches that value measured at the mouth only when metabolism is in a steady-state condition and consecutive end-expiratory lung volumes are precisely equal. However, ΔVO_{2_iS} and ΔVCO_{2_iS} are rarely zero when considering a

single breathing cycle, and therefore changes in the lung gas stores must be considered for valid estimation of alveolar-capillary gas transfer over the i^{th} breath (i.e., VO_{2_iA} and VCO_{2_iA}) (2).

Changes in lung gas stores depend on the changes in the lung volume and alveolar gas fractions (1–3):

$$\Delta VO_{2_iS} = V_{Li-1} \cdot \left(F_{AO_{2_i}} - F_{AO_{2_{i-1}}}\right) + F_{AO_{2_i}} \cdot \Delta V_{Li} \quad (9)$$

$$\Delta VCO_{2_iS} = V_{Li-1} \cdot \left(F_{ACO_{2_i}} - F_{ACO_{2_{i-1}}}\right) + F_{ACO_{2_i}} \cdot \Delta V_{Li} \quad (10)$$

where V_{Li-1} is the end-expiratory lung volume; $F_{AO_{2_{i-1}}}$ and $F_{ACO_{2_{i-1}}}$ are the alveolar fractions of O_2 and CO_2 of the preceding breath (i.e., *i*-1), respectively; $F_{AO_{2_i}}$ and $F_{ACO_{2_i}}$ are the alveolar fractions of O_2 and CO_2 in the current breath *i*, respectively; and ΔV_{Li} is the change in the lung volume occurring over breath *i*. Therefore, the changes in the lung gas stores depend mainly on two factors: 1) changes in the overall alveolar gas fractions of O_2 and CO_2 between the beginning and the end of breath *i* (i.e., the first term on the right-hand side of Equations 9 and 10, $F_{AO_{2_i}} - F_{AO_{2_{i-1}}}$ and $F_{ACO_{2_i}} - F_{ACO_{2_{i-1}}}$, respectively), and 2) the changes in lung volume (i.e., the second term on the right-hand side of Equations 9 and 10, ΔV_{Li}).

ΔV_{Li} can be determined by assuming no alveolus-to-capillary N_2 exchange (i.e., $VN_{2A} = VN_{2M} - \Delta VN_{2S} = 0$; where VN_{2A} and VN_{2M} are the amounts of N_2 exchanged at the alveolus and mouth levels, respectively, and ΔVN_{2S} is the change in the volume of N_2 in the lung over a breathing cycle). By substituting ΔVN_{2S} into Equation 9 (i.e., $\Delta VN_{2S} = V_{Li-1} \cdot \left(F_{AN_{2_i}} - F_{AN_{2_{i-1}}}\right) + F_{AN_{2_i}} \cdot \Delta V_{Li}$), ΔV_{L_i} can be determined as follows:

$$\Delta V_{L_i} = \frac{VN_{2_iM} - V_{L_{i-1}}\left(F_{AN_{2_i}} - F_{AN_{2_{i-1}}}\right)}{F_{AN_{2_i}}} \quad (11)$$

where the amount of N_2 exchanged at the mouth level over the breath i (i.e., VN_{2_iM}) can be determined as follows:

$$VN_{2_iM} = \int_{t_{bi_i}}^{t_{ei_i}} F_{IN_2} \cdot \dot{V}_{in} \cdot \mathrm{d}t \; - \; \int_{t_{be_i}}^{t_{ee_i}} F_{EN_2} \cdot \dot{V}_{ex} \cdot \mathrm{d}t \quad (12)$$

Beaver et al. (4) proposed an alternative approach to determine ΔV_{Li}:

$$\Delta V_{L_i} = \frac{V_{in_i}\left(\frac{1-F_{IH_2O_i}}{1-F_{AH_2O_i}}\right) - V_{ex_i}\left(\frac{1-F_{EH_2O_i}}{1-F_{AH_2O_i}}\right) - VO_{2_iM} + VCO_{2_iM} + V_{L_{i-1}}\left[\left(F_{AO_{2_i}} - F_{AO_{2_{i-1}}}\right) + \left(F_{ACO_{2_i}} - F_{ACO2_{2_{i-1}}}\right)\right]}{1-F_{AO_{2_i}} - F_{ACO_{2_i}}} \quad (13)$$

where $\left(\frac{1-F_{IH_2O_i}}{1-F_{AH_2O_i}}\right)$ and $\left(\frac{1-F_{EH_2O_i}}{1-F_{AH_2O_i}}\right)$ account for the water vapor pressure in the inspired and expired volumes, respectively, and F_{AO_2} and F_{ACO_2} are alveolar fractions of O_2 and CO_2 of the breath i and preceding one (i.e., i-1). This approach presents some advantages. First, ΔV_{Li} can be expressed in terms of measured quantities, which is convenient from a computational perspective. Second, compared to Equation 11, the Beaver et al.'s approach is less prone to estimation errors when the inspired gas fractions are transiently changed. For instance, when the inspired F_{N_2} changes significantly, which may occur when manipulating inspired gas fractions (e.g., supplemental oxygen), the terms VN_{2_iM} and $V_{L_{i-1}}\left(F_{AN_{2_i}} - F_{AN_{2_{i-1}}}\right)$ in Equation 11 are large and nearly the same

in magnitude during a transient period. This will expose Equation 11 to a higher error sensitivity and, in some cases, it cannot be used (4).

The only quantity that remains to be determined is V_{Li-1}, which is not directly measurable using Equations 9, 10, 11, and 13. Therefore, a pre-determined value for V_{Li-1} must be chosen. In their pioneering work, Auchincloss et al. (3) proposed setting V_{Li-1} equal to the functional residual capacity (*FRC*) of the subject (hereinafter referred to as the A algorithm). Other research groups made the same assumptions, in which *FRC* was either directly determined prior to exercise (4, 7, 10) or indirectly estimated using predictive equations (31).

Wessel et al. (32) suggested that, since the quantity $F_{AO_{2_i}} - F_{AO_{2_{i-1}}}$(and $F_{ACO_{2_i}} - F_{ACO_{2_{i-1}}}$) is likely to be rather small, the term $V_{Li-1} \cdot \left(F_{AO_{2_i}} - F_{AO_{2_{i-1}}}\right)$ (and $V_{Li-1} \cdot \left(F_{ACO_{2_i}} - F_{ACO_{2_{i-1}}}\right)$) can be neglected; thus, V_{Li-1} can be assumed to equal 0 L. However, this approach was subsequently questioned by di Prampero and Lafortuna (11) who demonstrated that setting V_{Li-1} equal to 0 changes the alveolar gas exchange measure. Moreover, they also showed that selecting different values of V_{Li-1} leads to a change in the B-by-B estimation and variability of VO_{2_iA} and VCO_{2_iA} (Figure 2) (11).

Swanson (6) proposed an alternative approach based on the assumption that most of the B-by-B gas exchange variability at the mouth level is the result of B-by-B changes in lung gas stores. Swanson proposed selecting V_{Li-1} as the lung volume that yields the lowest B-by-B variability in gas exchange (ref). He defined this volume as the 'effective lung volume', which represents the end-expiratory lung volume that 'effectively' participates in alveolar gas exchange (a practical example of the 'effective lung volume' is shown in Figure 2C). Swanson's approach yields a lower B-by-B VO_{2A} and VCO_{2A} variability compared to that of the A algorithm (5), which might be particularly useful for detecting time-based events in gas exchange (such as the gas exchange threshold). Nevertheless, this technique has some limitations. Since the effective lung volume can

only be calculated *a posteriori*, this method does not allow for real-time monitoring of gas exchange. Moreover, when applied to the rest-exercise transition, this technique assumes a deterministic variation of FRC as a function of time, which is a questionable assumption (2). In addition, B-by-B variability in gas exchange are a result of both physiologic events, such as rhythmic changes in pulmonary capillary blood flow with the breathing and cardiac cycles and the consequence of computational artifacts. di Prampero and Lafortuna (11) pointed out that it is difficult to distinguish between these effects, and stressed the notion that a valid alveolar gas exchange measure largely relies on the validity of V_{Li-1} assessment on a B-by-B basis (11).

Busso and Robbins (5) suggested yet another alternative, which is also based on minimizing B-by-B variability in gas exchange; data suggest that it provides the lowest B-by-B VO_{2A} and VCO_{2A} variability (5). They proposed that $V_{Li-1} = FRC$ and assumed that the 'true' change in alveolar end-expiratory gas fraction (i.e., $F_{AO_{2_i}} - F_{AO_{2_{i-1}}}$ and/or $F_{ACO_{2_i}} - F_{ACO_{2_{i-1}}}$) lies between 0 and the change in end-tidal gas fraction (i.e., $F_{ETO_{2_i}} - F_{ETO_{2_{i-1}}}$ and/or $F_{ETCO_{2_i}} - F_{ETCO_{2_{i-1}}}$); implying that the 'true' alveolar O_2 and CO_2 exchange is compromised within those obtained using Wessel's and Auchincloss's approach. Using a nine-compartment, non-homogeneous, tidally ventilated and constantly perfused lung model that reproduces a realistic breathing pattern, Busso and Robbins elegantly tested the validity of this method. Although appealing, this method presents similar limitations to that of Swanson – primarily that the requirements for *a posteriori* processing prevents real-time monitoring of gas exchange. A detailed review on different V_{Li-1}-based algorithms designed to estimate B-by-B alveolar gas exchange can be found elsewhere (1, 2). However a central tenet and limitation of these flow-based approaches is measurement of V_{Li-1} that, as described above, is methodologically challenging and often unavailable.

FIGURE 2 NEAR HERE

289 Notably, the development of techniques based on optical reflectance motion analysis (i.e,
290 optoelectronic plethysmography, OEP) has enabled the accurate estimation of lung volumes at any
291 point of the breathing cycle and, in turn, the determination of changes in V_{Li-1} for each breath (7,
292 12, 30, 33, 34). However, when using OEP-based techniques, independent estimation of the vital
293 capacity (*VC*) and *FRC* is still required to estimate $\dot{V}O_{2A}$ and $\dot{V}CO_{2A}$ (7). Using this technique,
294 Aliverti et al. (7) showed that V_{Li-1} changes between the onset and end of exercise, suggesting that
295 the use of a constant value for V_{Li-1} would likely introduce an estimation error in the alveolar gas
296 exchange computation. Despite its robustness, this technique is not free from limitations. For
297 instance, the overall volume changes of the chest wall measured by OEP-based techniques can
298 include blood volume shifts inside and outside of the thorax compartment, which could introduce an
299 estimation error when assessing changes in V_{Li-1} (35, 36). This technique is certainly appealing;
300 however, its application is demanding, time-consuming, and requires measures of *VC* and *FRC*,
301 which represent the primary limitation of this approach.

302

303 **Different definitions of the breathing cycle in the B-by-B gas exchange analysis**

304 To circumvent the issues related to measurements of of V_{Li-1}, Grønlund (15) proposed a radically
305 different solution; however, this requires the breathing cycle to be redefined. Rather than
306 performing the integration of flow and gas fraction signals within the inspiration and expiration
307 phases, it is performed between two successive expirations with equal F_{O_2} (or F_{CO_2}) values,
308 typically in the alveolar phase (Figure 3); the important point to note is that these equal F_{O2} (or
309 F_{CO2}) values do not not necessarily occur in consecutive breaths, or necessarily at a common time
310 or lung volume during a subsequent breathing cycle (Figure 4, panel A). Thus, Grønlund defined a
311 single breathing cycle as the time interval between two equal points of F_{O_2} (or F_{CO_2}) on successive
312 expirations, i.e., $F_{O_2(t1)} = F_{O_2(t2)}$, where *t1* and *t2* are the time instants with two equal F_{O_2} values.
313 By Grønlund's definition, the time interval between *t1* and *t2* represents the total time of a given

breathing cycle, where *t1* is the start and *t2* is the end of a cycle, which can be (and commonly is) different from the time interval between the beginning of two consecutive inspiration phases (i.e., the conventional breathing cycle). Grønlund's astute solution makes the term $\left(F_{AO_{2_i}} - F_{AO_{2_{i-1}}}\right)$ of Equation 11 equal to 0; thus, V_{Li-1} can be omitted from the computation. Therefore, according to Grønlund's algorithm (hereinafter referred to as the G algorithm), the volume of O_2 exchanged at the alveolar level over breath *i* is reduced to:

$$VO_{2_iA} = \int_{t1_i}^{t2_i}\left(\dot{V}_{in} - \dot{V}_{ex}\right)\cdot F_{O_2}\cdot \mathrm{d}t - \int_{t1_i}^{t3_i}\left(\dot{V}_{in} - \dot{V}_{ex}\right)\cdot F_{N_2}\cdot F_{O_2(t1_i)}\cdot \left(F_{N_2\,(t1_i)}\right)^{-1}\cdot \mathrm{d}t - \int_{t2_i}^{t3_i}\dot{V}_{ex}\cdot F_{O_2(t1_i)}\cdot \mathrm{d}t \quad (14)$$

To note, only the variables marked with (*t1*) are constant values for the considered breath *i* (i.e., $F_{O_2(t1_i)}$ and $\left(F_{N_2\,(t1_i)}\right)^{-1}$, the fraction of O_2 and N_2 at the time instant *t1*), while the others change over time (i.e., $\dot{V}_{in}$, $\dot{V}_{ex}$, F_{O_2}, F_{N_2}, which are variables varying over time). As originally pointed out by Grønlund (15), Equation 14 is very similar to that proposed earlier by Beaver et al. 1981 (i.e., Equation A9 in (4)), with the substantial difference of how a single breathing cicle is identified.

According to Equation 7, Equation 14 can be rewritten as follows:

$$VO_{2_{i\,A}} = \int_{t1_i}^{t2_i}\left(\dot{V}_{in} - \dot{V}_{ex}\right)\cdot F_{O_2}\cdot \mathrm{d}t - F_{O_2(t1_i)}\cdot \Delta V_{L_i} \quad (15)$$

where,

335 $$\Delta V_{L_i} = \frac{\int_{t1_i}^{t3_i} (\dot{V}_{in} - \dot{V}_{ex}) \cdot F_{N_2} \cdot \mathrm{d}t}{F_{N_2(t1_i)}} - \int_{t2_i}^{t3_i} \dot{V}_{ex} \cdot \mathrm{d}t \quad (16)$$

336

337 The second term on the right-hand side of Equation 15 accounts for the lung gas storage,
338 where ΔV_{Li} can be determined from N_2 balance (Equation 16). $F_{N_2(t1_i)}$ corresponds to the N_2 gas
339 fraction at *t1* and is used as a reference value for identifying F_{N_2} at *t3* ($F_{N_2(t3_i)}$), such that $F_{N_2(t1_i)} =$
340 $F_{N_2(t3_i)}$ (Figure 3). Therefore, *t3* is identified using the F_{N_2} signal, which satisfies the condition
341 $F_{N_2(t1_i)} = F_{N_2(t3_i)}$. Thus, Equation 11 can be reduced to Equation 16, which represents the changes
342 in the alveolar volume occurring over the i^{th} breath. If *t3* does not temporally coincide with *t2*,
343 volume correction $\int_{t2_i}^{t3_i} \dot{V}_E \cdot \mathrm{d}t$ must be applied (Figures 3 and 6), a correction that assumes gas
344 exchange from $t2_i$ to $t3_i$ with a RER=1. Notably, straightforward modifications, which are not
345 described here for simplicity, makes it possibile to obtain VCO_{2A} (e.g., applying Eq 8, inverting the
346 subtraction of the inspired and expired volumes from $(\dot{V}_I - \dot{V}_E)$ to $(\dot{V}_E - \dot{V}_I)$ and considering the
347 F_{CO_2} instead of the F_{O_2} trace).

348

349 *FIGURE 3 NEAR HERE*

350

351 Therefore, according to the G algorithm (15) the intra-breath interval time of breath *i* is
352 defined as the time interval between two points on successive expirations in which the lung O_2
353 fractional concentration is the same, i.e., $F_{O_2(t1_i)} = F_{O_2(t2_i)}$ (Figure 3). Generally, *t1* is selected
354 within the second half of the first expiration after the dead space has fully expired (10, 37), where
355 the condition $F_{O_2(t1_i)} = F_{O_2(t2_i)}$ is satisfied (Figures 3 and 4) (10, 37). Since the condition
356 $F_{O_2(t1_i)} = F_{O_2(t2_i)}$ can be met several times within breath *i*, and selecting different *t1-t2* couples
357 may lead to different $\dot{V}O_{2A}$ and $\dot{V}CO_{2A}$ (15), it is also necessary to determine which *t1* and *t2*

should be chosen. Capelli et al. (10) proposed a robust technique to identify *t1-t2-t3*, which enables the reliable measurement of $\dot{V}O_{2A}$ (see Capelli et al. (10) for further details).

The condition $F_{O_2(t1_i)} = F_{O_2(t2_i)}$ may not be satisfied between two consecutive breaths. In such cases, the subsequent expiration phase (i.e., following two standard breathing cycles after the *i*th breath) can be used to satisfy the condition $F_{O_2(t1_i)} = F_{O_2(t2_i)}$, which results in integration over a longer time interval (Figure 4A) (10, 37). Although unlikely, a given reference value at *t1* may not be attained at *t2* over a long series of breaths, which would result in losing the breath considered (Figure 4B) (see Capelli et al. for further details) (10). This may occur during hyperventilation, where tachypnea increases the slope of the alveolar partial pressure of expired O_2 (and CO_2) (38) (see below for further details).

FIGURE 4 NEAR HERE

The use of the G algorithm presents some advantages over the use of other V_{Li-1}-dependent algorithms, especially when attempting to characterize the B-by-B alveolar gas exchange kinetics during the transition to or from different work rates. For instance, di Prampero and Lafortuna showed that the A algorithm is likely to be exposed to an estimation error of the duration of $\dot{V}O_{2A}$ Phase I during the rest-exercise transition, and the magnitude of this error is highly dependent on the accuracy of V_{Li-1} (11). They also showed that assuming V_{Li-1} equal to 0 (i.e., Wessel et al.'s approach) causes wide variability in the estimation of the duration of phase 1 compared with assuming V_{Li-1} equals FRC. This instability might be due to the failure of the assumption that V_{Li-1}= 0 to completely account for changes in lung gas stores (11). Moreover, by comparing the G and A algorithms at the onset of exercise in the moderate-intensity domain, Cautero et al. demonstrated that the time constant of phase 2 $\dot{V}O_{2A}$ kinetics (τ_2) obtained when using the A algorithm was systematically greater than that obtained with the G algorithm (34.3 ± 9.18s vs. 45.0

± 10.66s, respectively) (37). Notably, the authors found a positive correlation between τ_2 and V_{Li-1}, suggesting that choosing greater V_{Li-1} values leads to a systematic increase in $\dot{V}O_2$ τ_2. Indeed, increases in V_{Li-1} amplifies the contribution of $F_{AO_{2_i}} - F_{AO_{2_{i-1}}}$ (see Equation 9) and $F_{AN_{2_i}} - F_{AN_{2_{i-1}}}$ (see Equation 11) in the $\dot{V}O_{2A}$ computation, which results in $\dot{V}O_{2A}$ kinetic distortions (see Cautero et al. (37) and Capelli et al. (2) for further details). Therefore, the use of the G algorithm can help prevent distortions caused by inaccuracy in the estimation or measurement of V_{Li-1}. However, we note that the 'true' alveolar $\dot{V}O_2$ (and $\dot{V}CO_2$) kinetics are unknown. It may be possible to use simulations of gas flow traces with different kinetic features to elucidate which algorithm provides the most realistic response kinetic estimation (see below).

Cettolo and Francescato (16) recently proposed an alternative algorithm designed to measure alveolar gas exchange, which also circumvents the requirement to assess V_{Li-1} by redefining the breathing cycle. Rather than considering the intra-breath interval time using the condition $F_{O_2(t1_i)} = F_{O_2(t2_i)}$, the start and the end of each breath *i* are defined by satisfying the condition $\frac{F_{O_2(t1_i)}}{F_{N_2(t1_i)}} = \frac{F_{O_2(t2_i)}}{F_{N_2(t2_i)}}$ (or $\frac{F_{CO_2(t1_i)}}{F_{N_2(t1_i)}} = \frac{F_{CO_2(t2_i)}}{F_{N_2(t2_i)}}$), typically in the alveolar phase (Figure 5) (where *t1* and *t2* conceptually have the same meaning as *t1* and *t2* in Equation 14; see below for further details). Similar to the G algorithm, this condition makes the term $\left(F_{AO_{2_i}} - F_{AO_{2_{i-1}}}\right)$ of Equation 11 equal 0, allowing V_{Li-1} to be omitted from the computation. Thus, the breathing cycle can be defined as the time interval between two equal values of $\frac{F_{O_2}}{F_{N_2}}$ (or $\frac{F_{CO_2}}{F_{N_2}}$) on successive, but not necessarily consecutive, expiration phases.

Cettolo and Francescato (16) reorganized Equation 7, which is essentially the method proposed by Auchincloss et al. (3).

405 $$VO_{2_iA} = VO_{2_iM} - \frac{F_{AO_{2_i}}}{F_{AN_{2_i}}} \cdot VN_{2_iM} + V_{Li-1} \cdot \left(\frac{F_{AO_{2_{i-1}}} \cdot F_{AN_{2_i}} - F_{AO_{2_i}} \cdot F_{AN_{2_{i-1}}}}{F_{AN_{2_i}}} \right) \quad (17)$$

406

407 Considering the condition $\frac{F_{O_2(t1_i)}}{F_{N_2(t1_i)}} = \frac{F_{O_2(t2_i)}}{F_{N_2(t2_i)}}$, Equation 17 reduces to

408

409 $$VO_{2_iA} = \int_{t1_i}^{t2_i} \left(\dot{V}_I - \dot{V}_E\right) \cdot F_{O_2} \cdot \mathrm{d}t - \frac{F_{O_2(t1_i)}}{F_{N_2(t1_i)}} \cdot \int_{t1_i}^{t2_i} \left(\dot{V}_I - \dot{V}_E\right) \cdot F_{N_2} \cdot \mathrm{d}t \quad (18)$$

410

411 Equation 18 is a simplified version of Equation 15; straightforward modifications, which will
412 not be described here, make it possibile to also obtain alveolar CO_2 exchange. Notably, although *t1*
413 and *t2* in Equation 18 have the same conceptual meanings as *t1* and *t2* in Equations 14 and 15, they
414 are defined differently (i.e., $\frac{F_{O_2(t1_i)}}{F_{N_2(t1_i)}} = \frac{F_{O_2(t2_i)}}{F_{N_2(t2_i)}}$) (16) (Figures 3 and 5).

415

416 *FIGURE 5 NEAR HERE*

417

418 Equation 18 presents several advantages from a computational perspective. For instance, the
419 Cettolo and Francescato algorithm (hereinafter referred to as the CF algorithm) does not require the
420 definition of *t3*, which must be determined when using the G algorithm (Figure 5). Moreover,
421 identifying the breathing cycle using the FO_2/FN_2 and FCO_2/FN_2 ratio traces may help identify
422 outlier breaths. The FN_2 trace generally shows greater noise and signal distortion compared to the
423 FO_2/FN_2 and FCO_2/FN_2 ratio traces, which may affect the identification of *t1-t2-t3* (not present in
424 the CF algorithm). Furthermore, the FO_2/FN_2 and FCO_2/FN_2 ratio traces have signal amplitudes
425 that are greater than that of FN_2 alone, which may reduce variability associated with trace detection

in real time (16, 39). Nevertheless, the advantage of using FO_2/FN_2 and/or FCO_2/FN_2 ratio traces, instead of FO_2 and FN_2 and/or FCO_2 and FN_2, have yet to be determined by independent research groups under different exercise conditions and/or using different modalities (see below).

There are also limited data directly comparing the G and CF algorithms; thus, whether one algorithm can outperform the other is unclear. Some data suggest no differences in the alveolar B-by-B gas exchange estimation between the two algorithms; however, the comparison was performed over a limited range of $\dot{V}O_2$, $\dot{V}CO_2$, and ventilatory rates (16). Notably, the CF algorithm was only recently introduced; hence, there are limited data showing its validity in assessing B-by-B alveolar gas exchange compared to the G algorithm (16, 39–42). Therefore, further investigations are warrented, to better understand whether substantial differences exist between these algorithms, and which more accurately measures the true physiologic response.

Limitations, methodological considerations, and future directions

Employing the G or CF algorithms has the undoubted advantage of removing the need to measure V_{Li-1}, which is appealing from a practical perspective. However, redefining the breathing cycle for the B-by-B gas exchange analysis may present some limitations. First, as previously highlighted (1, 43), these techniques would benefit from validation conducted by independent research groups under different conditions. For instance, it would be of great interest to test these algorithms together, under different environmental conditions (e.g., hypoxia, hyperoxia), exercise modalities (e.g., running, cycling, walking), with different populations (e.g., patients with cardiovascular and lung diseases and athletes), body positions (e.g., supine and upright posture) or work rate protocols (e.g., square-wave, sinusoidal-wave, ramp- and step-incremental tests). Specifically, comparisons made under conditions where lung volumes, lung gas stores and/or ventilation-perfusion relationships are expected to vary would help to identify the algorithm that best characterizes the true physiologic response.

Second, Whipp et al. (43) pointed out that Grønlund's approach may provide a different breath duration under specific conditions, such as during the transition from rest to exercise, compared with that of the conventional flow-based approach. Since the slope of the alveolar partial pressure of expired O_2 (and CO_2) increase at the onset of exercise and during continued exercise (38), a particular intra-breath F_{O_2} reference value at *t1* might be reached earlier during the expiration phase at *t2*, which in turn would result in a shorter estimated breath duration, and differentially alter the durations of inspiratory and/or expiratory time (such as in t_I/t_E or t_I/t_{TOT}), than with the conventional approach (43). The same concern applies to the CF algorithm (16), although specific aspects of this algorithm may help mitigate this concern (see below) (39, 41). However, no study has investigated the potential differences in breath duration among different algorithms; therefore, further investigations are required.

Whipp et al. (43) also stated that during acute hyperventilation, due to the large increment of the entire F_{AO_2} (or fall in F_{ACO_2}), a given intra-breath F_{O_2} reference value at *t1* (or F_{CO_2}) may not match any F_{O_2} (or F_{CO_2}) value at *t2* in the expired phase, resulting in the potential loss of breath detection using the G algorithm (Figure 4B). This may negatively affect the analysis of gas exchange kinetics during the transition phases. Modifications in the CF algorithms may help reduce the influence of large changes in F_{O_2}/F_{N_2} (or F_{CO_2}/F_{N_2}) on the identification of the breathing cycle (39, 41). Cettolo and Francescato have recently implemented a technique in which each breathing cycle is identified without considering the end timepoint of the preceding cycle and the start timepoint of the following one (i.e., the so-called "independent breath" algorithm) (39, 41). Therefore, each breathing cycle has its own *t1* and *t2*, where *t1* of the breath *i*+1 does not necessarily correspond to *t2* of the breath *i* (i.e., non-contiguity in time of the breathing cycles, Figure 4C). This would increase the possibility of identifying the breathing cycle during outlying breaths (e.g., atpically large or small breaths such as a sigh or a pant) and reduce the negative effects of hyperventilation on the identification of the breathing cycle and gas exchange estimation

476 (39, 41). Although some promising findings have already been reported (39–42), utlization of this
477 approach would benefit from further validation by independent research groups under different
478 exercise conditions. Moreover, the impact of hyperventilation on gas exchange kinetics estimation
479 when using the G algorithm remains to be systematically determined.

480 Concerns have been raised regarding how ventilatory-based variables are computed using the
481 G and CF algorithms (1). Information is lacking regarding the inspired and expired volumes, which
482 are needed to estimate other important variables such as $\dot{V}_E$, $\dot{V}_I$, the ventilatory equivalents for O_2
483 and CO_2 (i.e., $\dot{V}_E/\dot{V}O_2$ and $\dot{V}_E/\dot{V}CO_2$, respectively), and inspiratory and expiratory time. However,
484 it is worth noting that several (if not all) ventilatory-based variables can be determined using these
485 approaches. The intra-breath integration of the positive flow signal values between *t1* and *t2* can
486 provide the expired volume (i.e., V_{ex}), which can be used to derive other variables (such as $\dot{V}_E$ and
487 V_T) (Figure 6). Likewise, the intra-breath integration of negative values can provide the inspired
488 volume (i.e., V_{in}), which in turn would enable the estimation of $\dot{V}_I$ (Figure 6). This procedure would
489 also theoretically enable the estimation of B_R, where T_{TOT} corresponds to the time period elapsing
490 between *t1* and *t2* (Figure 6). Inspiratory and expiratory times are also computable in the G and CF
491 algorithms, although their physiological meaning is questionable, as they do not refer to the start
492 and end of a conventional inspiration and expiration phase, which are commonly used to gain
493 insights into the mechanisms involved in the control of the transition phase between inspiration and
494 expiration, or vice-versa (27, 44, 45). However, although these ventilatory-based variables are
495 computable using the G and CF algorithms, they have not been reported in published works. It is
496 currently unclear whether these algorithms would provide a reasonable estimation of ventilatory-
497 based variables. Evaluation of variability and irregularity of ventilatory-based variables during
498 CPET has the potential to detect underlying breathing pattern disorders (46, 47). For instance,
499 Bansal et al. (48) showed that a $\dot{V}E$ approximate entropy (i.e., a measure of $\dot{V}_E$ variability) > 0.88
500 conferred sensitivity and specificity to detect breathing pattern disorder of 70% and 80%,

501 respectively. Whether this ventilatory-based information, computed using V_{Li-1}-independent
502 algorithms, provide the same valuable information is currently unknown. Further study is
503 recommended to demonstrate that *all* cardiopulmonary exercise testing (CPET) variables can be
504 precisely and accurately derived.

505

506 *FIGURE 6 NEAR HERE*

507

508 Similarly, quantitative analysis of ventilatory and gas exchange kinetics during exercise is
509 commonly used to understand underlying metabolic and ventilatory control mechanisms (43, 49)
510 and are modified in patients with chronic disease (50, 51). This is particularly true for the
511 investigation of the control mechanisms of $\dot{V}_E$, where analysis of $\dot{V}_E$ and $\dot{V}CO_{2A}$ kinetics can
512 provide important physiological information (52–56).

513 Analysis of other ventilatory-based variables can also provide useful information for athletes
514 and populations with chronic disease (56–58). For instance, $\dot{V}_E/\dot{V}O_2$ and $\dot{V}_E/\dot{V}CO_2$ responses can be
515 used to non-invasively identify the gas exchange threshold (59, 60) and for diagnostic and
516 prognostic stratification (57, 61). Therefore, identifying the most appropriate and reliable way to
517 quantify ventilatory-based variables is of paramount importance.

518 The impact of lung gas store changes on B-by-B alveolar O_2 and CO_2 exchange rates during
519 progressive exercise (i.e., step-wise or ramp-incremental work-rate protocols) has received less
520 attention compared to the responses occurring during square-wave work-rate protocols (reviewed in
521 (2)). Since progressive exercise is commonly used in research and clinical evaluation, it is of
522 paramount importance to understand whether the dynamic changes in the alveolar gas stores affect
523 the B-by-B gas exchange and their derived variables (such as gas exchange threshold and the
524 ventilatory equivalent for O_2 and CO_2). Indeed, the use of $\dot{V}O_{2A}$ and $\dot{V}CO_{2A}$ instead of $\dot{V}O_{2M}$ and
525 $\dot{V}CO_{2M}$ was shown to increase the B-by-B signal-to-noise ratio and reduce B-by-B variability (4, 7,

10–12), thereby potentially improving discrimination of time-based events in gas exchange. However, there are no studies exploring the effect of using different algorithms on threshold detection.

Mathematical simulations and mechanical gas exchange simulation systems may be used to assess the validity of different alveolar corrections on the measurements of gas exchange and kinetics. As previously mentioned, the 'real' alveolar gas exchange kinetics is unknown. Although speculative, simulating gas flow traces with different known kinetics could potentially help to compare different algorithms to identify the algorithm that provides the most accurate kinetic estimates. On the other hand, the use of mechanical gas exchange simulation systems could be employed to assess the validity of alveolar gas exchange measures during steady-state conditions and in the presence of an aberrant single breath (42). The application of these techniques seems feasible (5, 42, 62), but the paucity of studies using these approaches means that further investigation is needed.

Since $\dot{V}O_{2A}$ and $\dot{V}CO_{2A}$ can be obtained using different reference values at *t1*, *t2* or *t3* (depending on the algorithm used – G or CF), a given breathing cycle obtained for $\dot{V}O_{2A}$ is not temporally aligned with that for $\dot{V}CO_{2A}$. Moreover, T_I, T_E and T_{TOT} may not necessarily have the same durations when computed by these difference algorthims. Therefore, a temporal misalignment on a B-by-B basis between $\dot{V}O_{2A}$ and $\dot{V}CO_{2A}$, although small, can occur. This issue can be partially overcome by interpolation and extrapolation. Second-by-second interpolation and extrapolation (rather than B-by-B) of data are commonly used in post-processing when investigating gas exchange kinetics of actual (52, 63, 64) and simulated data (53, 65). Although, again, the implications for altering the standard reporting format for research and clinical gas exchange and ventilatory variables has yet to be determined. Moreover, interpolation/extrapolation techniques might alter the data, especially during the rest-exercise transition period, potentially affecting the physiological interpretation.

551 Until recently, G and CF algorithms have typically only been applied to raw gas flow and gas
552 concentration recordings post-processing. That is, they have not been used to provide a real-time B-
553 by-B measure of gas exchange. However, the use of the CF algorithm in real-time data analysis is
554 feasible (39). The CF algorithm can identify *t1* and *t2* within every single breath in real time as data
555 are collected (39). Thus, similar to what occurs during the classical real-time analysis of gas
556 exchange, the integration of flow and gas fractions can be performed independently in a single
557 breath (the so-called "independent breath"), allowing real-time data visualization (39, 41). Although
558 not yet tested, this modification could theoretically be implemented in the G algorithm. Further
559 studies are required to identify the most efficient technical solution to implement these algorithms
560 in automated real-time B-by-B systems.

561

562 **A call to action**

563 Data show the clear advantages of using $\dot{V}O_{2A}/\dot{V}CO_{2A}$ instead of $\dot{V}O_{2M}/\dot{V}CO_{2M}$ in B-by-B gas
564 exchange analysis. However, the requirement for substantial validation work that confirms the
565 advantage of V_{Li-1}-independent algorithms to determine not only alveolar gas exchange, but also
566 ventilatory-based variables, is prohibitive to making use of these routines. For example, it is still
567 unclear which alveolar correction better reflects alveolar-to-capillary gas exchange, especially
568 under the diverse range of conditions commonly observed in research and clinical CPET
569 laboratories. In addition, the lack of open access to these algorithms for routine application is a key
570 barrier limiting the use of alveolar corrections. We are unaware of any automated commercial
571 system that has implemented an algorithm to measure B-by-B alveolar gas exchange. This is despite
572 literature that shows the advantages of using $\dot{V}O_{2A}$ /$\dot{V}CO_{2A}$ instead of $\dot{V}O_{2M}$ /$\dot{V}CO_{2M}$ increases
573 signal-to-noise and reduces distortions in gas exchange responses during exercise. Therefore, given:
574 (i) the introduction of the algorithm by Auchincloss et al. in 1966 (3); (ii) the development of
575 several solutions aimed at optimizing the estimation of alveolar gas exchange (2, 41); and (iii) the

large number of studies showing the importance of differentiating between $\dot{V}O_{2M}/\dot{V}CO_{2M}$ and $\dot{V}O_{2A}/\dot{V}CO_{2A}$ (2, 4–6, 10, 16, 30, 37, 40, 41, 66); it is surprising that manufacturers have not progressed past conventional B-by-B algorithms and developed commercial systems that provide alveolar gas exchange analysis alongside standard measurements. This would not only increase signal-to-noise to provide improved characterization of clinically-important variables from an exercise test, but would also enable implementation of the most suitable algorithm for a given purpose, satisfying a wide range of different needs in health and chronic disease. Incorporating different algorithms into commercial systems would advance the reach of these techniques and facilitate the progression of our knowledge on their validity and applicability under different exercise conditions.

Perspectives and Significance

Although fundamental concerns have been raised in using alternative algorithms that change the definition of the breathing cycle, their benefit for increasing accuracy and precision of alveolar gas exchange measurement is appealing and promising. Nevertheless, the paucity of data describing the physiologic meaning of several ventilatory-based variables when using these alternative algorithms requires further investigation. In addition, further validation studies are required to assess these methods and their implementation in real-time for online analysis. This is essential to understand which algorithm best characterizes the 'true' physiological response in both clinical and research settings.

Glossary

BTPS	Body Temperature, ambient Pressure, and Saturated water vapor
CPET	Cardiopilmonary exercise testing
CO_2	Carbon dioxide
$\dot{V}_E$, $\dot{V}_I$	Expired flow rate, inspired flow rate
$\dot{V}_{in}$, $\dot{V}_{ex}$	Flow rate during inspiration and expiration, respectively
F_{AO_2}, F_{ACO_2}, F_{AN_2}, F_{AH_2O}	Alveolar gas concentrations
F_{EO_2}, F_{ECO_2}, F_{EN_2}, F_{EH_2O}	Fractional gas concentration in expirate
F_{ETO_2}, F_{ETCO_2}	End-tidal gas fraction
F_{IO_2}, F_{ICO_2}, F_{IN_2}, F_{IH_2O}	Fractional gas concentration in inspirate
$F_{N_2(t3)}$	Fractional N_2 concentration at the time instant *t3*
$F_{O_2(t1)}$, $F_{CO_2(t1)}$, $F_{N_2(t1)}$	Fractional gas concentration at the time instant *t1*

$F_{O_2(t2)}$, $F_{CO_2(t2)}$, $F_{N_2(t2)}$	Fractional gas concentration at the time instant *t2*
FRC	Functional residual capacity
N_2	Nitrogen
OEP	Optoelectronic plethysmography
O_2	Oxygen
RER	Respiratory exchange ratio
STPD	Standard Temperature and barometric Pressure, Dry
t_{TOT}, t_{in}, t_{ex}	Time interval of a breath, inspiratory time interval, expiratory time interval
VC	Vital capacity
$\dot{V}_E/\dot{V}O_2$, $\dot{V}_E/\dot{V}CO_2$	Ventilatory equivalents for O_2 and CO_2, respecvively
V_{in}, V_{ex}	Inspired volume, expired volume
V_{Li}	end-expiratory lung volume of the i^{th} breath
V_{Li-1}	end-expiratory lung volume of the preceding breath
VO_{2A}, VCO_{2A}	Alveolar-to-capillary gas exchange volume
$\dot{V}O_{2A}$, $\dot{V}CO_{2A}$	Alveolar-to-capillary gas exchange rate
VO_{2M}, VCO_{2M}, VN_{2M}	Pulmonary gas exchange volume
$\dot{V}O_{2M}$, $\dot{V}CO_{2M}$	Pulmonary gas exchange rate
V_T, B_R	Tidal volume, breathing rate
ΔV_{Li}	Changes in lung volume during breath interval
ΔVO_{2S}, ΔVCO_{2S}, ΔVN_{2S}	Changes in lung gas content during breath interval

τ_2	Time constant of phase II gas kinetic

Acknowledgements

The authors are very grateful to Professor Pietro Enrico di Prampero who critically read the manuscript and provided valuable comments and suggestions.

Author contributions

Conception or design of the work: M.G., C.G., W.W.S., H.B.R., R.C., C.F., and C.C.. Acquisition, analysis or interpretation of data for the work: M.G., C.G., W.W.S., H.B.R., R.C., C.F., and C.C.. M.G. wrote the first draft of the manuscript. All the Authors revisited the work critically for important intellectual content. All authors approved the final version of the manuscript and agreed to be accountable for all aspects of the work in ensuring that questions related to the accuracy or integrity of any part of the work are appropriately investigated and resolved. All persons designated as authors qualify for authorship, and all those who qualify for authorship are listed.

Funding

Harry B. Rossiter is supported by grants from NIH (R01HL151452, R01HL153460, P50HD098593, R01DK122767) and the Tobacco Related Disease Research Program (T31IP1666).

Competing interest

Harry B. Rossiter reports consulting fees from Omniox Inc., and is involved in contracted clinical research with Boehringer Ingelheim, GlaxoSmithKline, Novartis, AstraZeneca, Astellas, United Therapeutics, Genentech and Regeneron. He is a visiting Professor at the University of Leeds, UK. Richard Casaburi is involved in contracted research with United Therapeutics, Genentech, and Regeneron. He is an advisory board member for Inogen and Abbott and a speaker bureau member for GlaxoSmithKline. Carrie Ferguson is involved in contracted clinical research with United Therapeutics, Genentech, and Regeneron. She is a visiting Associate Professor at the University of Leeds, UK.

References

1. **Ward SA**. Open-circuit respirometry: real-time, laboratory-based systems. *Eur J Appl Physiol* 118: 875–898, 2018.
2. **Capelli C**, **Cautero M**, **Pogliaghi S**. Algorithms, modelling and VO_2 kinetics. *Eur J Appl Physiol* 111: 331–342, 2011.
3. **Auchincloss JH Jr**, **Gilbert R**, **Baule GH**. Effect of ventilation on oxygen transfer during early exercise. *J Appl Physiol* 21: 810–818, 1966.
4. **Beaver WL**, **Lamarra N**, **Wasserman K**. Breath-by-breath measurement of true alveolar gas exchange. *J Appl Physiol* 51: 1662–1675, 1981.
5. **Busso T**, **Robbins PA**. Evaluation of estimates of alveolar gas exchange by using a tidally ventilated nonhomogenous lung model. *J Appl Physiol* 82: 1963–1971, 1997.
6. **Swanson GD**. Breath-to-breath considerations for gas exchange kinetics. In: *Exercise, Bioenergetics and Gas Exchange*, edited by P Cerretelli And B J Whipp. Amsterdam, Elsevier/north-Holland, 1980, p. 211–222.
7. **Aliverti A**, **Kayser B**, **Macklem PT**. Breath-by-breath assessment of alveolar gas stores and exchange. *J Appl Physiol* 96: 1464–1469, 2004.
8. **Giezendanner D**, **Cerretelli P**, **Di Prampero PE**. Breath-by-breath alveolar gas exchange. *J Appl Physiol* 55: 583–590, 1983.

9. **Lumb AB**, **Thomas CR**. *Nunn's Applied Respiratory Physiology eBook: Nunn's Applied Respiratory Physiology eBook*. Elsevier Health Sciences, 2020.

10. **Capelli C**, **Cautero M**, **di Prampero PE**. New perspectives in breath-by-breath determination of alveolar gas exchange in humans. *Pflugers Arch* 441: 566–577, 2001.

11. **di Prampero PE**, **Lafortuna CL**. Breath-by-breath estimate of alveolar gas transfer variability in man at rest and during exercise. *J Physiol* 415: 459–475, 1989.

12. **Wüst RCI**, **Aliverti A**, **Capelli C**, **Kayser B**. Breath-by-breath changes of lung oxygen stores at rest and during exercise in humans. *Respir Physiol Neurobiol* 164: 291–299, 2008.

13. **Lumb AB**, **Nunn JF**. Respiratory function and ribcage contribution to ventilation in body positions commonly used during anesthesia. *Anesth Analg* 73: 422–426, 1991.

14. **Henke KG**, **Sharratt M**, **Pegelow D**, **Dempsey JA**. Regulation of end-expiratory lung volume during exercise. *J Appl Physiol* 64: 135–146, 1988.

15. **GrØnlund J**. A new method for breath-to-breath determination of oxygen flux across the alveolar membrane. *Eur J Appl Physiol Occup Physiol* 52: 167–172, 1984.

16. **Cettolo V**, **Francescato MP**. Assessment of breath-by-breath alveolar gas exchange: an alternative view of the respiratory cycle. *Eur J Appl Physiol* 115: 1897–1904, 2015.

17. **Beaver WL**, **Wasserman K**, **Whipp BJ**. On-line computer analysis and breath-by-breath graphical display of exercise function tests. *J Appl Physiol* 34: 128–132, 1973.

18. **Macfarlane DJ**. Automated metabolic gas analysis systems. *Sports Med* 31: 841–861, 2001.

19. **Beaver WL**. Water vapor corrections in oxygen consumption calculations. *J Appl Physiol* 35: 928–931, 1973.

20. **Macfarlane DJ**. Open-circuit respirometry: a historical review of portable gas analysis systems. *Eur J Appl Physiol* 117: 2369–2386, 2017.

21. **Porszasz J**, **Stringer W**, **Casaburi R**. Equipment, measurements and quality control. In: *Clinical Exercise Testing*, edited by Paolo Palange, Pierantonio Laveneziana, J. Alberto Neder, Susan A. Ward. ERS | Monograph, 2018, p. 59–81.

22. **Bradley PW**, **Younes M**. Relation between respiratory valve dead space and tidal volume. *J Appl Physiol* 49: 528–532, 1980.

23. **Garcia-Tabar I**, **Eclache JP**, **Aramendi JF**, **Gorostiaga EM**. Gas analyzer's drift leads to systematic error in maximal oxygen uptake and maximal respiratory exchange ratio determination. *Front Physiol* 6: 308, 2015.

24. **Porszasz J**, **Blonshine S**, **Cao R**, **Paden HA**, **Casaburi R**, **Rossiter HB**. Biological quality control for cardiopulmonary exercise testing in multicenter clinical trials. *BMC Pulm Med* 16: 13, 2016.

25. **Sietsema KE**, **Stringer WW**, **Sue DY**, **Ward S**. *Wasserman & Whipp's: Principles of Exercise Testing and Interpretation: Including Pathophysiology and Clinical Applications*. Lippincott Williams & Wilkins, 2020.

26. **Feldman PM**. find_cross.m, version 2.1 [Online]. *MATLAB Central File Exchange*: [date unknown]. https://www.mathworks.com/matlabcentral/fileexchange/24063-find_cross-m-version-2-1 [Retrieved April 23 2022].

27. **Roux SG**, **Garcia S**, **Bertrand B**, **Cenier T**, **Vigouroux M**, **Buonviso N**, **Litaudon P**. Respiratory cycle as time basis: an improved method for averaging olfactory neural events. *J Neurosci Methods* 152: 173–178, 2006.

28. **Boutellier U**, **Kündig T**, **Gomez U**, **Pietsch P**, **Koller EA**. Respiratory phase detection and delay determination for breath-by-breath analysis. *J Appl Physiol* 62: 837–843, 1987.

29. **Hlastala MP**, **Wranne B**, **Lenfant CJ**. Cyclical variations in FRC and other respiratory variables in resting man. *J Appl Physiol* 34: 670–676, 1973.

30. **Aliverti A**, **Kayser B**, **Cautero M**, **Dellacà RL**, **di Prampero PE**, **Capelli C**. Pulmonary V˙O2 kinetics at the onset of exercise is faster when actual changes in alveolar O2 stores are considered. *Respir Physiol Neurobiol* 169: 78–82, 2009.

31. **Brambilla I**, **Pizzamiglio R**. *ABC dei test di Funzionalità Respiratoria (ABC of Respiratory Function Testing)*. Masson, Milan, 1979.

32. **Wessel HU**, **Stout RL**, **Bastanier CK**, **Paul MH**. Breath-by-breath variation of FRC: effect on VO2 and VCO2 measured at the mouth. *J Appl Physiol* 46: 1122–1126, 1979.

33. **Cala SJ**, **Kenyon CM**, **Ferrigno G**, **Carnevali P**, **Aliverti A**, **Pedotti A**, **Macklem PT**, **Rochester DF**. Chest wall and lung volume estimation by optical reflectance motion analysis. *J Appl Physiol* 81: 2680–2689, 1996.

34. **LoMauro A**, **Colli A**, **Colombo L**, **Aliverti A**. Breathing patterns recognition: A functional data analysis approach. *Comput Methods Programs Biomed* 217: 106670, 2022.

35. **Aliverti A**, **Pedotti A**. Opto-electronic plethysmography. *Monaldi Arch Chest Dis* 59: 12–16, 2003.

36. **Iandelli I**, **Aliverti A**, **Kayser B**, **Dellacà R**, **Cala SJ**, **Duranti R**, **Kelly S**, **Scano G**, **Sliwinski P**, **Yan S**, **Macklem PT**, **Pedotti A**. Determinants of exercise performance in normal men with externally imposed expiratory flow limitation. *J Appl Physiol* 92: 1943–1952, 2002.

37. **Cautero M**, **Beltrami AP**, **di Prampero PE**, **Capelli C**. Breath-by-breath alveolar oxygen transfer at the onset of step exercise in humans: methodological implications. *Eur J Appl Physiol* 88: 203–213, 2002.

38. **Steinacker JM**, **Dehnert C**, **Whipp BJ**. Effect of exercise intensity on the changes in alveolar slopes of carbon dioxide and oxygen expiratory profiles in humans. *Eur J Appl Physiol* 85: 56–61, 2001.

39. **Cettolo V**, **Francescato MP**. Assessing breath-by-breath alveolar gas exchange: is the contiguity in time of breaths mandatory? *Eur J Appl Physiol* 118: 1119–1130, 2018.

40. **Koschate J**, **Cettolo V**, **Hoffmann U**, **Francescato MP**. Breath-by-breath oxygen uptake during running: Effects of different calculation algorithms. *Exp Physiol* 104: 1829–1840, 2019.

41. **Francescato MP**, **Cettolo V**. The "independent breath" algorithm: assessment of oxygen uptake during exercise. *Eur J Appl Physiol* 119: 495–508, 2019.

42. **Francescato MP**, **Thieschäfer L**, **Cettolo V**, **Hoffmann U**. Comparison of different breath-by-breath gas exchange algorithms using a gas exchange simulation system. *Respir Physiol Neurobiol* 266: 171–178, 2019.

43. **Whipp BJ**, **Ward SA**, **Rossiter HB**. Pulmonary O2 uptake during exercise: conflating muscular and cardiovascular responses. *Med Sci Sports Exerc* 37: 1574–1585, 2005.

44. **Ramirez J-M**, **Baertsch N**. Defining the Rhythmogenic Elements of Mammalian Breathing. *Physiology* 33: 302–316, 2018.

45. **Feldman JL**. Neurophysiology of breathing in mammals. In: *Handbook of Physiology. The Nervous System. Intrinsic Regulatory Systems of the Brain*. Washington, DC: Am Physiol Soc, 1986, p. 9, 463–524.

46. **Boulding R**, **Stacey R**, **Niven R**, **Fowler SJ**. Dysfunctional breathing: a review of the literature and proposal for classification. *Eur Respir Rev* 25: 287–294, 2016.

47. **Ionescu MF**, **Mani-Babu S**, **Degani-Costa LH**, **Johnson M**, **Paramasivan C**, **Sylvester K**, **Fuld J**. Cardiopulmonary Exercise Testing in the Assessment of Dysfunctional Breathing. *Front Physiol* 11: 620955, 2020.

48. **Bansal T**, **Haji GS**, **Rossiter HB**, **Polkey MI**, **Hull JH**. Exercise ventilatory irregularity can be quantified by approximate entropy to detect breathing pattern disorder. *Respir Physiol Neurobiol* 255: 1–6, 2018.

49. **Forster HV**, **Haouzi P**, **Dempsey JA**. Control of breathing during exercise. *Compr Physiol* 2: 743–777, 2012.

50. **Rossiter HB**. Exercise: Kinetic considerations for gas exchange. *Compr Physiol* 1: 203–244, 2011.

51. **Ward SA**. Ventilatory control in humans: constraints and limitations. *Exp Physiol* 92: 357–366, 2007.

52. **Girardi M**, **Nicolò A**, **Bazzucchi I**, **Felici F**, **Sacchetti M**. The effect of pedalling cadence on respiratory frequency: passive vs. active exercise of different intensities. *Eur J Appl Physiol* 121: 583–596, 2021.

53. **Girardi M**, **Gattoni C**, **Mauro L**, **Capelli C**. The effects of sinusoidal linear drifts on the estimation of cardiorespiratory dynamic parameters during sinusoidal workload forcing: a simulation study. *Respir Physiol Neurobiol* 289: 103652, 2021.

54. **Casaburi R**, **Whipp BJ**, **Wasserman K**, **Koyal SN**. Ventilatory and gas exchange responses to cycling with sinusoidally varying pedal rate. *J Appl Physiol* 44: 97–103, 1978.

55. **Casaburi R**, **Whipp BJ**, **Wasserman K**, **Beaver WL**, **Koyal SN**. Ventilatory and gas exchange dynamics in response to sinusoidal work. *J Appl Physiol* 42: 300–301, 1977.

56. **Ward SA**. Ventilation/carbon dioxide output relationships during exercise in health. *Eur Respir Rev* 30, 2021. doi: 10.1183/16000617.0160-2020.

57. **Levett DZH**, **Jack S**, **Swart M**, **Carlisle J**, **Wilson J**, **Snowden C**, **Riley M**, **Danjoux G**, **Ward SA**, **Older P**, **Grocott MPW**, **Perioperative Exercise Testing and Training Society (POETTS)**. Perioperative cardiopulmonary exercise testing (CPET): consensus clinical

guidelines on indications, organization, conduct, and physiological interpretation. *Br J Anaesth* 120: 484–500, 2018.

58. **Beaver WL**, **Wasserman K**, **Whipp BJ**. A new method for detecting anaerobic threshold by gas exchange. *J Appl Physiol* 60: 2020–2027, 1986.

59. **Reinhard U**, **Müller PH**, **Schmülling RM**. Determination of anaerobic threshold by the ventilation equivalent in normal individuals. *Respiration* 38: 36–42, 1979.

60. **Whipp BJ**, **Ward SA**, **Wasserman K**. Respiratory markers of the anaerobic threshold. *Adv Cardiol* 35: 47–64, 1986.

61. **Puente-Maestu L**, **Palange P**, **Casaburi R**, **Laveneziana P**, **Maltais F**, **Neder JA**, **O'Donnell DE**, **Onorati P**, **Porszasz J**, **Rabinovich R**, **Rossiter HB**, **Singh S**, **Troosters T**, **Ward S**. Use of exercise testing in the evaluation of interventional efficacy: an official ERS statement. *Eur Respir J* 47: 429–460, 2016.

62. **Swanson GD**, **Sherrill DL**. A model evaluation of estimates of breath-to-breath alveolar gas exchange. *J Appl Physiol* 55: 1936–1941, 1983.

63. **Cautero M**, **di Prampero PE**, **Tam E**, **Capelli C**. Alveolar oxygen uptake kinetics with step, impulse and ramp exercise in humans. *Eur J Appl Physiol* 95: 474–485, 2005.

64. **Lamarra N**, **Whipp BJ**, **Ward SA**, **Wasserman K**. Effect of interbreath fluctuations on characterizing exercise gas exchange kinetics. *J Appl Physiol* 62: 2003–2012, 1987.

65. **Benson AP**, **Bowen TS**, **Ferguson C**, **Murgatroyd SR**, **Rossiter HB**. Data collection, handling, and fitting strategies to optimize accuracy and precision of oxygen uptake kinetics estimation from breath-by-breath measurements. *J Appl Physiol* 123: 227–242, 2017.

66. **Cautero M**, **di Prampero PE**, **Capelli C**. New acquisitions in the assessment of breath-by-breath alveolar gas transfer in humans. *Eur J Appl Physiol* 90: 231–241, 2003.

807
808
809
810
811
812
813
814
815
816
817
818
819
820

821 **Figure captions**

822 **Figure 1**. Flow (panel A), partial pressure of oxygen (panel B) and partial pressure of carbon
823 dioxide (panel C) during a series of breaths peformed at a moderate exercise intensity in healthy-
824 trained individual. The upper panel also depicts the zero-crossing points (open circle) identified
825 using the MATLAB function "find_cross.m" (26).

826 **Figure 2.** Single breath alveolar $\dot{V}O_2$ (panel A) and $\dot{V}CO_2$ (panel B) exchange as a function of
827 ventilation computed on the same breath (continuous lines). $\dot{V}O_{2M}/\dot{V}O_{2A}$ vs $\dot{V}_I$ (panel A) and
828 $\dot{V}CO_{2M}/\dot{V}CO_{2A}$ vs $\dot{V}_E$ (panel B). Continuous lines (calculated on 100 breaths) depict differences
829 from the expected value in alveolar gas exchange when using different $V_{Li\text{-}1}$ values (from 0 to 5 L)
830 in Eqs 7 and 7. The dashed line depicts gas exchange at mouth ($\dot{V}O_{2M}$ in panel A and $\dot{V}CO_{2M}$ in
831 panel B). Panel C shows the variability of alveolar $\dot{V}O_2$ (open square) and $\dot{V}CO_2$ (filled square)
832 expressed as coefficient of variation (c.v., %), as a function of different $V_{Li\text{-}1}$ values. The $V_{Li\text{-}1}$ value

833 which gives the lowest computed $\dot{V}O_{2A}$ and $\dot{V}CO_{2A}$ variability is indicated by vertical arrows and
834 ELV_{min} (effective lung volume; i.e., $ELV_{min,O2}$ and $ELV_{min,CO2}$, respectively). FRC (functional
835 residual capacity) indicates when V_{Li-1} = FRC. (Used and modified by permission; di Prampero and
836 Lafortuna Breath-by-breath estimate of alveolar gas transfer variability in man at rest and during
837 exercise. 1989. *J. Physiol.* 415, 459–475).

838 **Figure 3.** Partial pressure of O_2 and N_2 in mmHg (PO_2 and PN_2, respectively) (top panel). The same
839 data over a single respiratory cycle i.e., between the 5th and the 13th second (bottom panel). Exp_{i-1},
840 $Insp_i$, and Exp_i refer to the conventional expiration phase of the breath *i-1*, inspiration phase of the
841 breath *i* and expiration phase breath *i*. t_d indicates the time after which the estimated dead space gas
842 volume is fully expired. The reference value *t1* is chosen according to specific criteria (see text and
843 Capelli et al. 2001 (10) for further details), while *t2* and *t3* are chosen to yield PO_2 and PN_2 equal to
844 *t1,* respectively. The respiratory cycle is defined as the time period elapsing between *t1* and *t2*.
845 (Used by permission; Capelli C, Cautero M, di Prampero PE. New perspectives in breath-by-breath
846 determination of alveolar gas exchange in humans. *Pflugers Arch*. 2001;441(4):566–77.)

847 **Figure 4.** Panel A shows a particular case where a given F_{O2} reference value at the time instant *t1*
848 does not meet any F_{O2} value on the successive expiration to satisfy the condition $F_{O_2(t1_i)} = F_{O_2(t2_i)}$,
849 but during which a value equal to $F_{O_2(t1_i)}$is then met during the subsequent expiration. This results
850 in an integration of gas and flow data over a longer time interval. The horizontal dotted line shows
851 that the latest F_{O2} value pertaining to the second expiration that coincides with the first F_{O2} value
852 would allow the identification of a respiratory cycle using the G algorithm. Panel B shows the effect
853 of hyperventilation on FO_2 (O_2 fractional concentration in %) during three successive expirations.
854 There are no F_{O2} reference values at time instant *t1* that are met on two consecutive expirations,
855 making the identification of a respiratory cycle using the G algorithm impossible. Panel C depicts
856 the so-called "independent breath" algorithm, which allows the identification of two respiratory
857 cycles ($t1_i$-$t2_i$ and $t1_{i+1}$-$t2_{i+1}$) during hyperventilation. FO_2/FN_2 ratio (ratio of O_2 and N_2 fractions in

%). Here the summed duration of two successive breaths is larger than the summed duration of two conventional breaths defined by the beginning of two consecutive inspiration phases i.e. consecutive breaths overalp. See text for further details.

Figure 5. Comparison of Grønlund's and Cettolo & Francescato's algorithms. Upper and middle panels show the method introduced by Grønlund, which is also described in Figure 3. The bottom panel depicts the method introduced by Cettolo and Francescato (16). For the Cettolo and Francescato's method, the reference value *t1* is chosen accordingly to specific criteria (see text and Cettolo and Francescato, 2015 (16) for details), while *t2* is chosen to yield FO_2/FN_2 equal to *t1*. The respiratory cycle is defined as the period time elapsing between *t1* and *t2*. (Used by permission; Cettolo V, Francescato MP. Assessment of breath-by-breath alveolar gas exchange: an alternative view of the respiratory cycle. *Eur J Appl Physiol*. 2015;115(9):1897–904.)

Figure 6. A single respiratory cycle identified using the Grønlund's algorithm, where *t1* and *t2* represent the beginning and the end of one breath. The upper panel shows the gas flow at the mouth. The expiration occurs during positive deflections of the flow signal, while the inspiration occurs during negative deflections of the flow signal. The lower panel shows the fractional O_2 concentration. The soft dotted area represents the inspired gas volume, while the heavy dotted area corresponds to the expired gas volume. The thick line represents the gas flow occurring between *t3* and *t2* (i.e., the volume correction for Equation 16). Some ventilatory-based variables estimated over *t1* and *t2* are as following: V_{ex}= 0.9 L STPD (V_T= 1.2 L BTPS), V_{in}=1.03 L STPD, $\dot{V}_E$ = 23 L · min^{-1} STPD, $\dot{V}_I$= 24 L · min^{-1} STPD. The alveolar net transfer of oxygen uptake occurring over *t1* and *t2* is equal to $\dot{V}O_{2A}$ = 1.09 L · min^{-1} STPD. The time elapsing between *t1* and *t2* (i.e., T_{TOT}, which is the total time of the considered breath) is equal to 2.54 s. The corresponding breathing frequency is 24 breaths· min^{-1}.

Table 1. General definition of breathing cycle (in the time domain) when using classic (V_{Li-1}-based algorithms), Grønland, and Cettolo and Francescato algorithms to estimate alveolar gas transfer.

	Classic approach	G algorithm	CF algorithm
	V_{Li-1}-based algorithms	V_{Li-1}-independent algorithms	
Definition of breathing cycle (in time domain)	Time interval between the beginning of two consecutive inspiration phases	Time interval between two equal values of FO_2 (or FCO_2) on successive, but not necessarily consecutive, expiration phases, typically in the alveolar phase	Time interval between two equal values of FO_2/FN_2 (or FCO_2/FN_2) on successive, but not necessarily consecutive, expiration phases, typically in the alveolar phase
Signal(s) used to identify the breathing cycle	Flow signal	FO_2, FCO_2, and FN_2	FO_2, FCO_2, and FN_2
Variables required to obtain alveolar gas transfer	Flow signal, FO_2, FCO_2, FN_2, and V_{Li-1}	Flow signal, FO_2, FCO_2, and FN_2	Flow signal, FO_2, FCO_2, and FN_2

Abbreviations: V_{Li-1}, end-expiratory lung volume; G, Grønland algorithm; CF, Cettolo and Francescato algorithm; FO_2, oxygen fraction; FCO_2, carbon dioxide fraction; FN_2, nitrogen fraction.

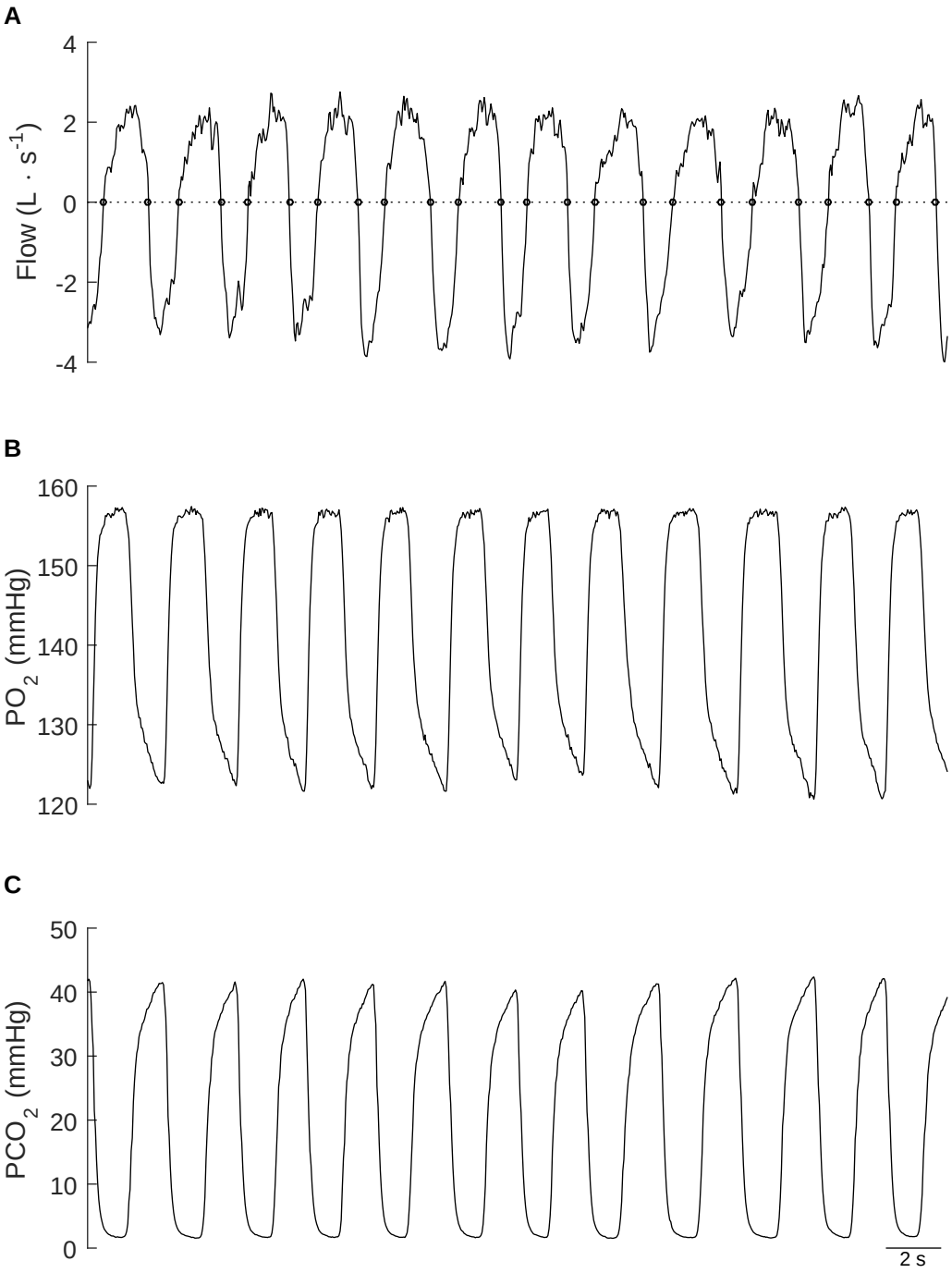
A
4
2
0
-2
-4
Flow (L · s-1)
B
160
150
140
130
120
PO2 (mmHg)
C
50
40
30
20
10
0
PCO2 (mmHg)
2 s

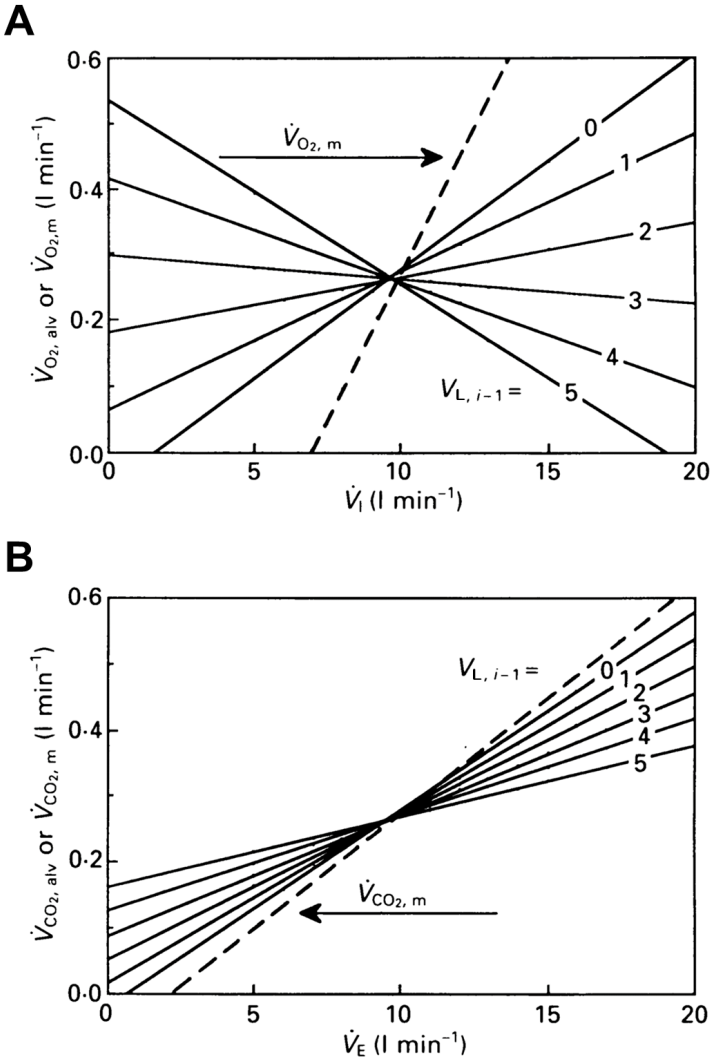
A
0·6
0·4
0·2
0·0
0
5
10
15
20
$\dot{V}_{O_2,\,alv}$ or $\dot{V}_{O_2,m}$ (l min^{-1})
$\dot{V}_I$ (l min^{-1})
$\dot{V}_{O_2,\,m}$
0
1
2
3
4
5
$V_{L,\,i-1}$ =
B
0·6
0·4
0·2
0·0
0
5
10
15
20
$\dot{V}_{CO_2,\,alv}$ or $\dot{V}_{CO_2,\,m}$ (l min^{-1})
$\dot{V}_E$ (l min^{-1})
$V_{L,\,i-1}$ =
0
1
2
3
4
5
$\dot{V}_{CO_2,\,m}$
C
40
30
20
10
0
c.v. of $\dot{V}_{O_2}$ or $\dot{V}_{CO_2}$ (%)
$V_{L,\,i-1}$= 0
$ELV_{min,\,O_2}$
$ELV_{min,\,CO_2}$
FRC
0
1
2
3
4
5
$V_{L,\,i-1}$ (l)

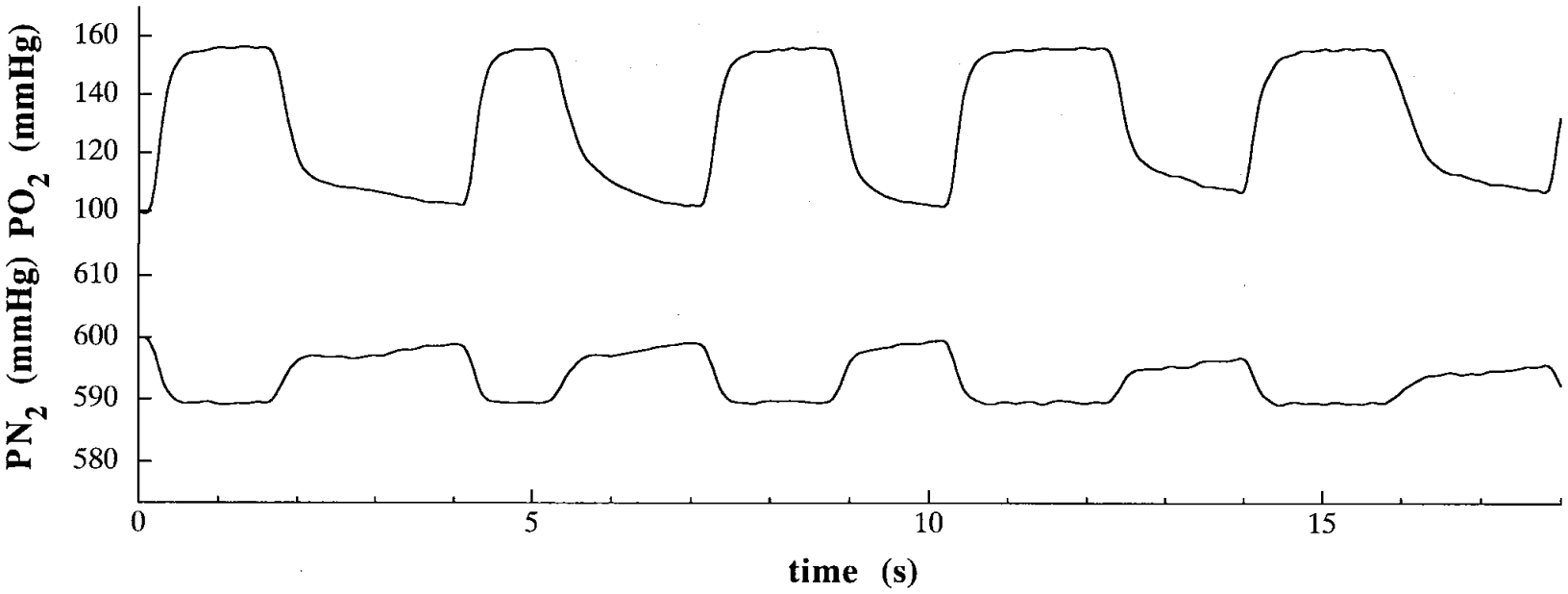
PN2 (mmHg) PO2 (mmHg)
160
140
120
100
610
600
590
580
0
5
10
15
time (s)

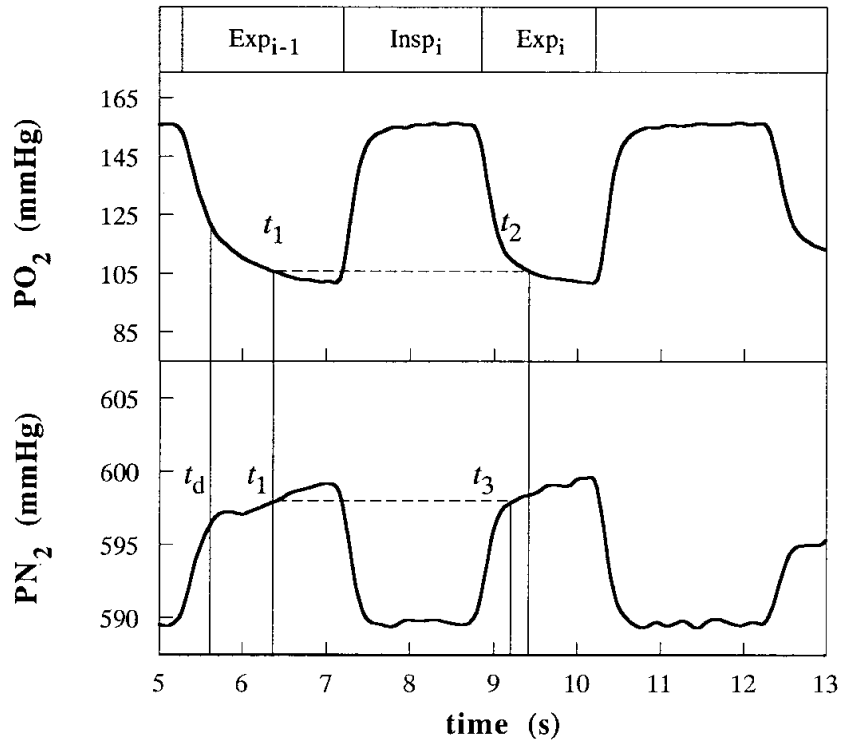
Exp i-1
Insp i
Exp i
PO2 (mmHg)
165
145
125
105
85
t1
t2
PN2 (mmHg)
605
600
595
590
td
t1
t3
5
6
7
8
9
10
11
12
13
time (s)

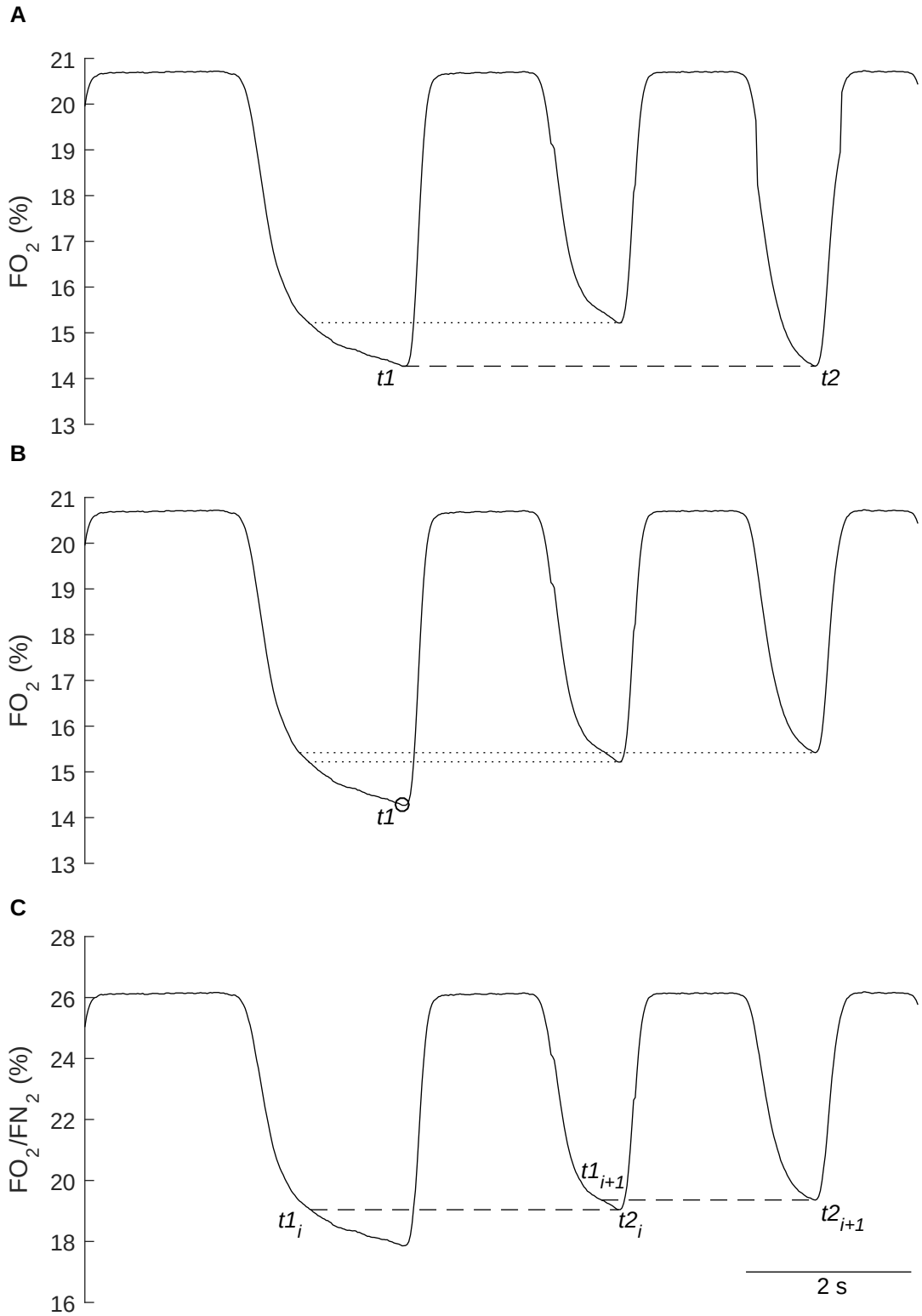
A
21
20
19
18
17
16
15
14
13
FO2 (%)
t1
t2
B
21
20
19
18
17
16
15
14
13
FO2 (%)
t1
C
28
26
24
22
20
18
16
FO2/FN2 (%)
t1i
t2i
t1i+1
t2i+1
2 s

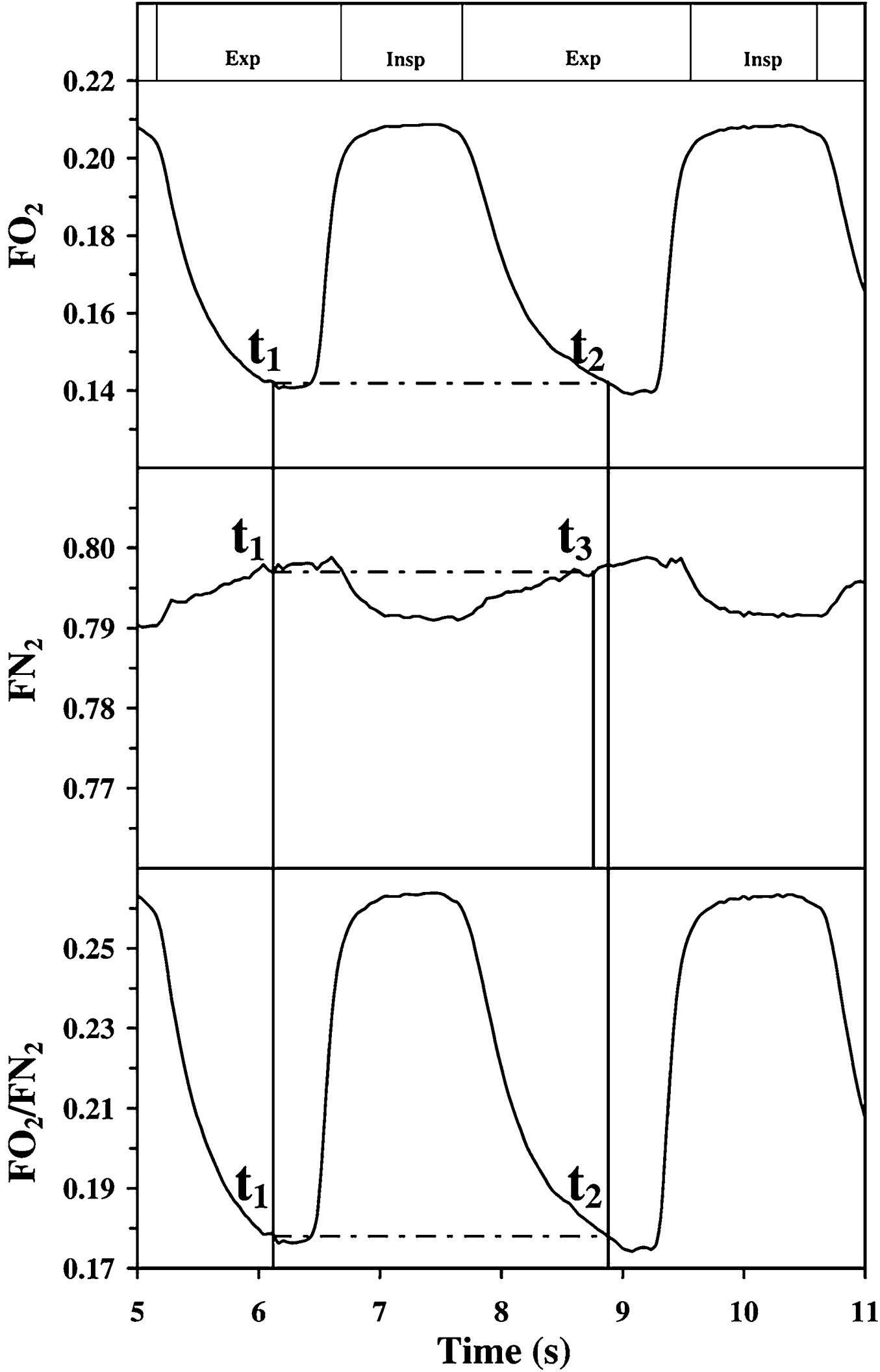
Exp
Insp
Exp
Insp
0.22
0.20
0.18
0.16
0.14
FO2
t1
t2
0.80
0.79
0.78
0.77
FN2
t1
t3
0.25
0.23
0.21
0.19
0.17
FO2/FN2
t1
t2
5
6
7
8
9
10
11
Time (s)

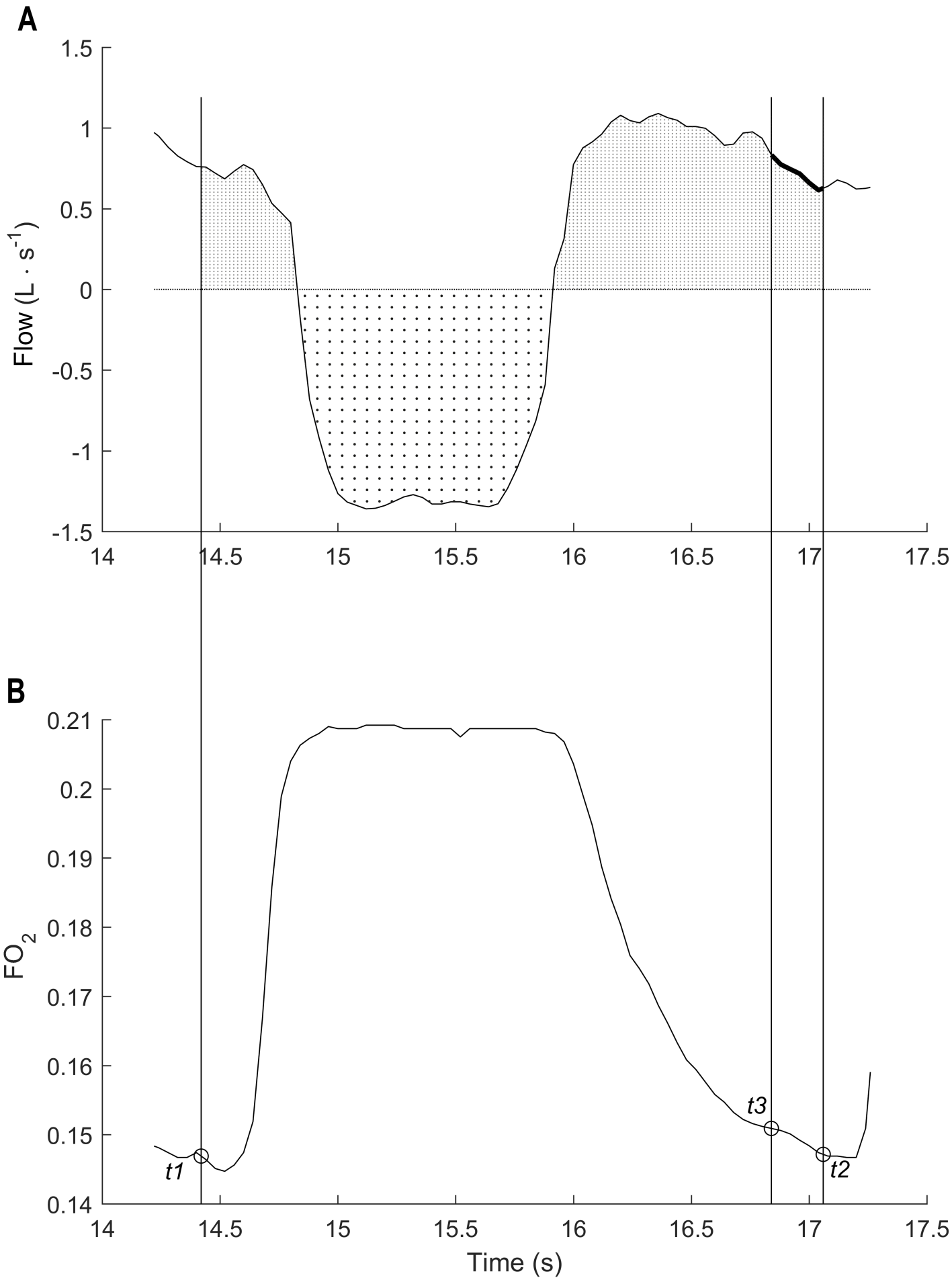
A
1.5
1
0.5
0
-0.5
-1
-1.5
Flow (L · s-1)
14
14.5
15
15.5
16
16.5
17
17.5
B
0.21
0.2
0.19
0.18
0.17
0.16
0.15
0.14
FO2
t1
t2
t3
Time (s)